



## FRAGILITY FUNCTIONS FOR NON-ENGINEERED MASONRY DWELLING IN PERU

M. Suarez<sup>(1)</sup>, Y. Maruyama<sup>(2)</sup>, C. Zavala<sup>(3)</sup>, M. Diaz<sup>(4)</sup>, C. Moya<sup>(5)</sup>

<sup>(1)</sup> Research Assistant, Japan-Peru Center for Earthquake Engineering Research and Disaster Mitigation (CISMID),  
[msuarez@uni.edu.pe](mailto:msuarez@uni.edu.pe)

<sup>(2)</sup> Assoc. Professor, Graduate School of Engineering, Chiba University - Japan, [ymaruyam@faculty.chiba-u.jp](mailto:ymaruyam@faculty.chiba-u.jp)

<sup>(3)</sup> Assoc. Professor, National University of Engineering, [czavala@uni.edu.pe](mailto:czavala@uni.edu.pe)

<sup>(4)</sup> Assoc. Professor, National University of Engineering, [mdiazf@uni.edu.pe](mailto:mdiazf@uni.edu.pe)

<sup>(5)</sup> PhD. Candidate, Chiba University – Japan, [lmoyah@chiba-u.jp](mailto:lmoyah@chiba-u.jp)

### **Abstract**

In order to contribute to mitigate the impact of future earthquakes, appropriate measures to protect human life should be taken into account, therefore the estimation of vulnerability must be an important issue. This article proposes fragility functions for typical two-story confined masonry dwellings made of representative tubular clay bricks in Peru. One of those is non-retrofitted dwelling and another is retrofitted by wire mesh and plaster mortar.

Fragility curves showed 50% of probability that the non-retrofitted dwelling will get collapse from 300gals of PGA unlike the retrofitted dwelling, which will get collapse from 650 gals. Also the non-retrofitted dwelling suggests that smaller increment in strong ground motion will result in higher probability of damage, which is reduced by the improvement of retrofitting of wire mesh and plaster mortar.

*Keywords: Confined masonry, retrofitting, non-engineered, fragility functions.*



## 1. Introduction

The human losses around the world from earthquakes are mostly common due to the collapse of dwellings thus the low capacity against lateral loads does not give enough time for people to escape.

In developing countries like Peru, the informality to build dwellings in urban areas is increasing. In Lima city, new emerging districts with no urban planning policy are under development. The main structural system is confined masonry of clay bricks. However, many people live in non-engineered dwellings (low quality of materials, irregularities, unfavorable soil conditions, etc.). Damages in this kind of structures by the last earthquakes showed their high vulnerability.

## 2. Background

Peru is one of countries located on the Ring of Fire (81% of the seismic activity in the world, USGS) so the country has been exposed to seismic risk. The history shows us that more than 250 years have passed since the last mega earthquake in 1746 and more than 40 years since the last significant one in 1974. In both cases, the capital, Lima, has been directly affected.

For the last five decades, Lima has continually experienced a large urbanization process, where 9 million approximately, one third of Peru's population, live. People move to the capital looking for better style life, resulting in the establishment of new emerging districts with no urban planning policy. They relocated non-suitable soil to construct, like valley areas or deserted rocky foothills close to the historical center [1]. In this context, a large number of non-engineered dwellings were built, creating a big risk upon the occurrence of earthquake. According to the National Institute of Statistical and Informatics of Peru [2], more than 60% of total dwellings use confined masonry walls as structural system as it is show in the Fig. 1.



Fig. 1 – Non-engineered dwellings of masonry in emerging towns of Lima

### 2.1 Previous studies

The Japan-Peru Center for Earthquake Engineering Research and Disaster Mitigation (CISMID), based on Miranda, 1999, adopted a method to determine the seismic vulnerability in masonry buildings. The seismic response of buildings (estimation of inter-story displacement and drift) is calculated considering the maximum strong ground accelerations from studies in situ and the catalog of representative typologies buildings in specific areas. The criteria method or empirical method is based on several experimental test developed in the Structural Laboratory and developed by CISMID through the years.

In 2010, Japanese government through Japanese Science and Technology Agency (JST) and the Japanese International Cooperation Agency (JICA), support the project of research disaster mitigation by earthquake and tsunami in Peru named Science Association for Technology Research for Sustainable Development (SATREPS).



CISMID and Japanese researchers from Chiba University. There were groups to exchange knowledge in different areas as geotechnics, tsunamis, buildings, damage assessment and disaster mitigation plan.

Matsuzaki, 2013 evaluated the seismic vulnerability of buildings after the 2007 Pisco earthquake using damage survey data (more than 10,000) of masonry (71%) and adobe (16%) low-rise dwellings affected, where 72% were one-story buildings and 23% were two-story buildings; and simulated seismic ground motions. The fragility curves for brick masonry structures were compared with unreinforced masonry in Istanbul, within the range of 0.56g to 0.65g. The damage ratio was 20% larger than that in Pisco [3].

L. Quiroz, 2014 evaluated the seismic performance of residential buildings constructed of confined masonry walls in Lima by analytical fragility functions for dwellings from 1 to 3 stories at three hazard levels two story dwellings have a 36% probability of severe damage for occasional earthquakes and less than 5% of collapse for rare earthquakes and three story dwellings will suffer extensive damage even under occasional earthquakes. In addition, a retrofitting procedure involving the use of electro welded wire mesh was evaluated numerically. This procedure reduced the expected damage of two-story dwellings [4].

### 3. Behavior of masonry walls

#### 3.1 Experimental test

In order to evaluate the behavior of non-engineered masonry walls in Peru, in 2015 two experiments were carried out at Structural Laboratory of Japan-Peru Center for Earthquake Engineering Research and Disaster Mitigation (CISMID) by the support of Peruvian government through Ministry of Economy and Finance with Program 0068 [5].

Two full-scale confined masonry walls were tested, namely as Specimen 1 and Specimen 2. Both walls were 2400mm long by 2500mm of total high, with confining reinforced concrete of columns and beam (compressive strength  $f'_c=17\text{MPa}$  and yield strength  $f'_y=420\text{MPa}$ ) and the masonry wall of tubular bricks (compressive strength  $f'_m=2.2\text{MPa}$ ). Additionally, the Specimen 2 was retrofitted by wire mesh of 4mm diameter wire welded bar every 100mm long, commercial named Q-139, and 22.5mm thick of plaster mortar of 1:4 cement and sand ratio (compressive strength  $f'_m=15\text{MPa}$ ). This procedure was applied in both faces of the wall.

The result obtained from these experiments are shown in the Figure 1, the backbone represent the relationship between the applied load and displacement at the top of masonry wall. The red line is the backbone curve of the non-retrofitted masonry wall, Specimen 1, Also the blue line represent the backbone of the retrofitted masonry wall, Specimen 2.

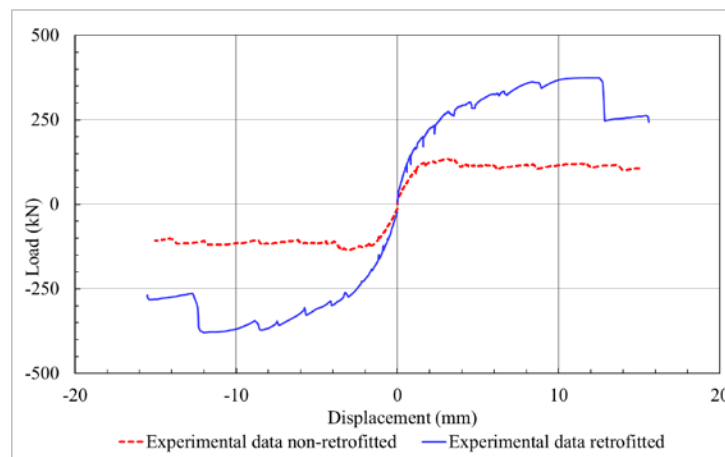


Fig. 2 – Envelope curve of Specimen 1 and Specimen 2



### 3.2 Numerical model of specimens

In order to obtain the closest characteristics of hysteretic results from Specimen 1 and Specimen 2, the software Stera3D v.4.0 was used [6].

The quad linear hysteresis model are applied to represent the behavior of the full-scale masonry walls. The hysteretic model is based on a degrading trilinear model in in terms of stiffness under cracking, yielding and maximum condition and based on parameters that controlled the shape of the model as stiffness degrading ratio (between 0-1), slip stiffness ratio (between 0-1) and strength degrading ratio (0-1), following the hysteresis loop ruler and equations provided in the technical manual of the software.

Six models were analyzed in order to evaluate the behavior of the full scale specimen tested. The Table 1 show the parameters that had good agreement regarding ductility, stiffness degradation and equivalent damping for each case. The Analytical model 1 represent the behavior of the Specimen 1 and the Analytical model 2 represent the behavior of the Specimen 2.

Table 1 – Parameters of analytical model

Parameters	<b>K0</b> (kN/mm)	<b>K1</b> (kN/mm)	<b>K2</b> (kN/mm)	<b>K3</b> (kN/mm)	<b>Fc</b> (kN)	<b>Fy</b> (kN)	<b>Fm</b> (kN)	$\alpha$	$\beta$	$\gamma$
Analytical model 1	130.67	52.27	20.83	-2.56	58.80	98.00	131.32	0.37	0.00	0.02
Analytical model 2	175.00	60.45	14.25	-12.88	137.20	267.54	396.46	0.58	0.00	0.05

Note:  $\alpha$  is stiffness degrading ratio,  $\beta$  is slip stiffness ratio and  $\gamma$  is strength degrading ratio.

Fig. 3 shows the hysteresis curves of experimental data and the analytical models, the red and blue dashed line was develop with the parameters of the Table 1.

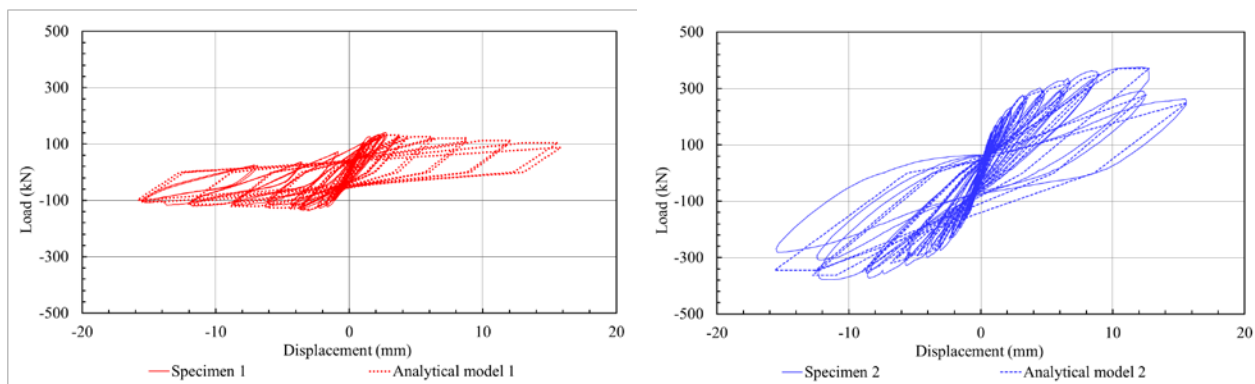


Fig. 3 – Hysteretic curve of specimens and analytical models

## 4. Seismic performance of typical dwelling

### 4.1 Numerical model of typical dwelling

Most dwellings of confined masonry walls in Lima have a rectangular shape. The walls distribution of the dwelling shown in the Fig. 4 was considered as the typical story [7], the area of this dwellings is around 90m<sup>2</sup>. The longitudinal direction has wall density ratio of 2%, on the other hand, the transversal direction has 5%.

Two numerical simulations of non-engineered dwellings were developed using [6]. The Dwelling 1, represent the model of two stories dwelling with non-retrofitted masonry walls, the properties of these walls

follow the parameters of the Analytical model 1; the Dwelling 2 represent the model of two stories dwelling with retrofit masonry walls using the parameters of the Analytical model 2.

The natural period using equation in the Peruvian Seismic Design Code NTE- E030-2016 is around 0.08s for two stories dwelling, and the natural periods from the numerical models were around 0.12s and 0.11s for the Dwelling 1 and Dwelling 2 respectively.

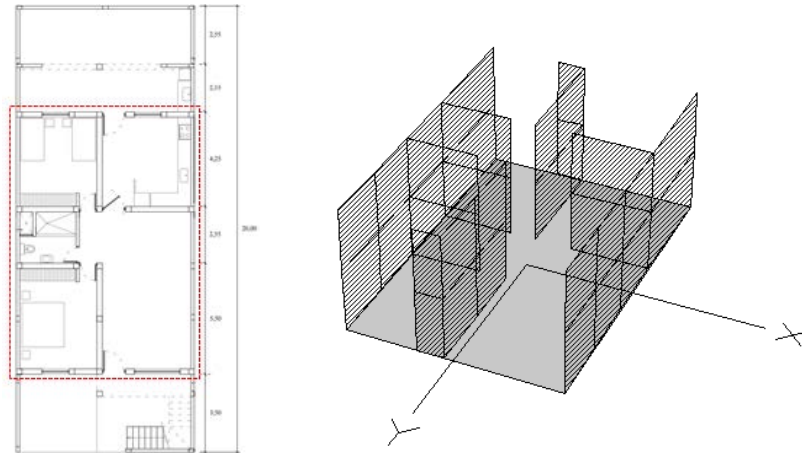


Fig. 4 – Peruvian dwelling [7]

#### 4.2 Strong ground motion

The strong motions used in this research were the recompilation of five records of synthetic strong ground motion records through SATREPS project. Based on historical earthquakes in southern Peru, a methodology for characterized source models of mega thrust earthquakes was developed.

According to the Peruvian Seismic Design Code NTE-E030-2013, there are three classifications for the kind of soil in Peru, the soil S1 is characterized by rock and sand and is considered good soil, soil S2 is an intermediate soil, soil S3 is a flexible soil with low shear strength.

The synthetic records were scaled for three kinds of soil, S1, S2 and S3, according to Peruvian Seismic Design Code NTE-E030-2013 by CISMID in 2014. [8].

Five scaled synthetic records for intermediate soil S2 were used, the horizontal components were considered separately as input in longitudinal direction as it shows the Table 2.

Table 2 – Record of synthetic strong ground motion

Station	PGA (gals)				
	CMD	PQR	EMO	DHN	VSV
East - West	509	517	479	510	468
North -South	459	493	510	474	494

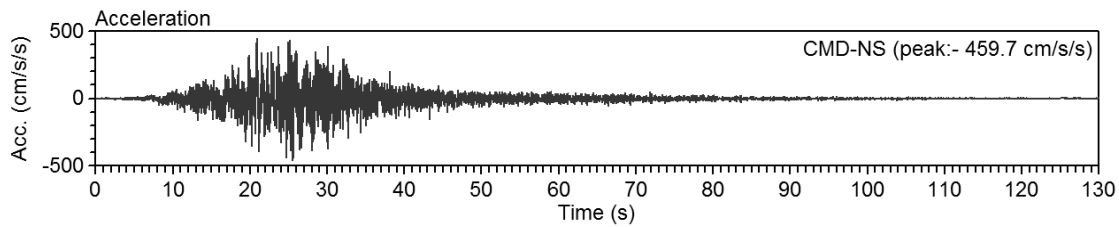


Fig. 5 – Time-history of CMD station

According to Quiroz [4], the strong ground motion parameter (eg. PGA, PGV and VSI) that shows highest correlation with damage index of a two-story numerical model is the PGA.

In order to obtain the fragility functions, the records for input strong ground motion were scaled from 50 gals of PGA to 1,000 gals at an interval of 10 gals, here in after amplified strong ground motion. As Bommer et al., recommended, the maximum parameter for scaling the strong ground motion should be three times of PGA (in this particular case) of the original records [9].

Also the frequency characteristics were checked. Fourier spectra was made in order to compare the frequency obtained from the original record and those who were scaled. As an example, the frequency of the original record of CMD station of North-South (CMD-NS) component was around 5.99 Hz, as shown in Fig. 6 and the frequency of scaled records for each 10 gals were 6.00 Hz.

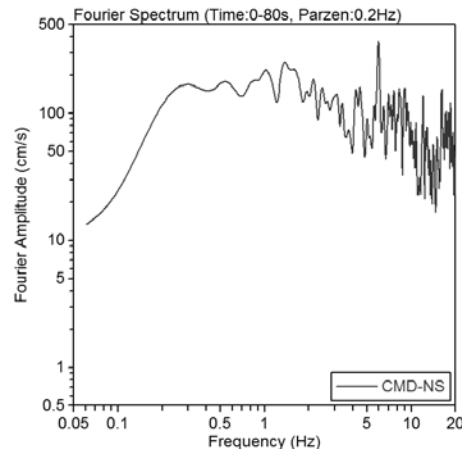


Fig. 6 – Fourier spectrum of CMD record wave

### 4.3 Response of typical dwelling

The damage of structures could be measured by the maximum deformation, ductility ratio, maximum drift, etc. In this study, the parameter to estimate the damage due to seismic scenarios will be the maximum drift at the top of the height story of typical dwellings.

In 2004, a full scale of two story masonry dwelling of hand-made solid clay bricks was carried out in the Structure Laboratory of the Japan-Peru Center for Earthquake Engineering Research and Disaster Mitigation, CISMID. From this experiment, Zavala et al. found the drifts in each stage of the test. At 1/800 drift, the diagonal cracks started in the wall, at 1/400 drift the initial cracking in the columns and the opening of diagonal cracking in the wall was observed, high deterioration on columns and wall were observed at 1/200 drift [10]. Based in this experiment, Quiroz [4], considered damage states in terms of drifts.

Table 3 – Damage states in terms of drift



Damage state	No damage (ND)	Light (L)	Severe (S)	Collapse (C)
Inter-story drift (%)	0 – 0.125	0.125 -0.286	0.286 – 0.500	>0.500

From dynamic analysis of two numerical models, Dwelling 1 and Dwelling 2, and using synthetic amplified ground motion as an input, the structures response was analyzed in terms of drift and classified following the damages state of the Table 3. These result are grouped in categories, in X axis; the synthetic sub-strong ground motion and in Y axis; the count of damages due to these scenarios.

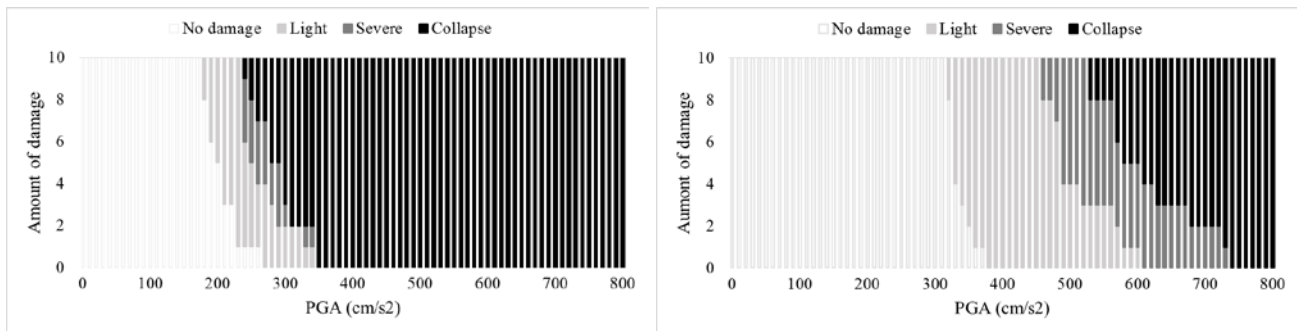


Fig. 7 – Damage obtained from Dwelling 1 and Dwelling 2

The Fig. 7 show the evolution of damage according to the increment of PGA for numerical models, left graph represent the damages of Dwelling 1, which show light damage state produced by 180gals of PGA, followed by the severe damage with 240gals, also in this level the collapse state continued until 350gals, where 100% of collapse damage was observed; right graph represent the Dwelling 2, the first light damage is observed at 320gals PGA, and then at 460gals and 530gals, where the severe and collapse damage state were observed. Finally for 740gals of acceleration the model collapse due all strong ground motion records used.

### 5. Fragility functions

The fragility functions quantify the seismic risk of specific structural system and the probability of damages depending on earthquakes scenarios. Therefore, the assessment of seismic risk could be done by using fragility functions, these tools are important since the results obtained are used to make decisions in order to mitigate the damages generated by earthquakes.

The structural seismic behavior of buildings can be evaluated by fragility functions, which is defined by the probability that a specific structure exceeds a damage limit state determined by earthquakes scenarios, as show in Eq. (1), where  $P_{ik}$  is the conditional probability,  $x_i$  is the damage state,  $y_k$  is the strong ground motion index,  $X$  is the variable of damage state and  $Y$  the variable of strong ground motion index.

$$P_{ik} = P[X \geq x_i | Y = y_k] \tag{1}$$

The cumulative probability  $P_R$  of being exceeding a particular damage state is defined by Eq. (2), where  $\Phi$  is the standard cumulative normal distribution function,  $Y$  is the strong ground motion index,  $\lambda$  is the mean deviation of  $\ln Y$  and  $\zeta$  is the standard deviation of  $\ln Y$ .

$$P_R = \Phi \left[ \frac{\ln Y - \lambda}{\zeta} \right] \tag{2}$$

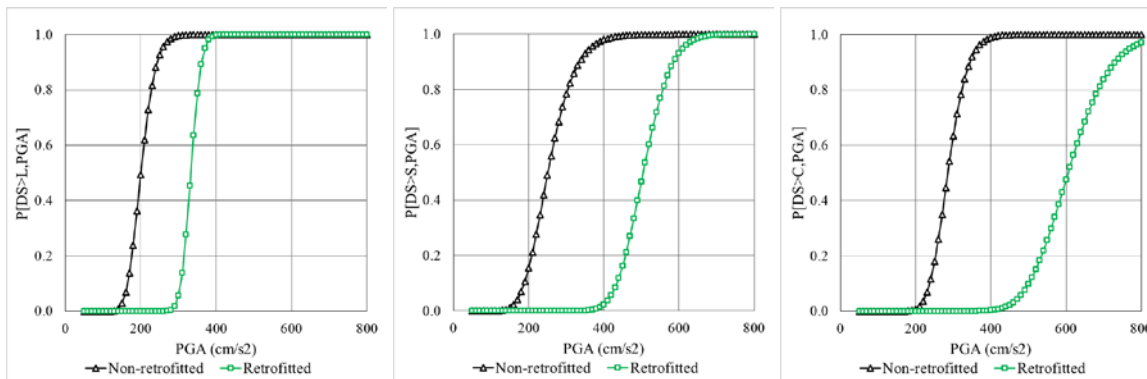


The mean and standard deviation ( $\lambda, \zeta$ ) were obtained from damages states calculated, the least-squares method was used to find the statistical parameters for each damage state plotting the logarithm of PGA and the inverse probability exceeding those damages, which is show in the Table 4.

Table 4 – Damage state of dwellings

Damage state	Dwelling 1 (non-retrofitted)		Dwelling 2 (retrofitted)	
	$\lambda$	$\zeta$	$\lambda$	$\zeta$
Light (L)	5.30	0.15	5.81	0.06
Severe (S)	5.53	0.22	6.22	0.12
Collapse (C)	5.65	0.15	6.41	0.15

The fragility functions were constructed using the cumulative probability PR of exceeding damage state defined before. In order to use Eq. (2), the lognormal probability distribution and the peak ground acceleration were plotted.



(a) Light damage state

(b) Severe damage state and

(c) Collapse damage state

Fig. 8 – Fragility functions

The Fig. 8 (a) and (b) show the comparison between the Dwelling 1 and Dwelling 2, represented by black and green line respectively, for the light and severe damage state. It can be seen that the structure performance was improved to double by retrofitting using wire mesh and plaster mortar in the simulated models. Dwelling 1 had 50% of probability to get light damage from strong ground motion of 200gals unlike Dwelling 2, which had 50% of probability from 300gals. In both cases, the slope of the fragility functions showed that for small difference of PGA, the structures had higher probability to get light damage. The 50% of probability to get severe damage for Dwelling 1 and Dwelling 2 were around 250gals and 500gals. In this case, the observed slope was not so much like in light damage, probably because of the contribution of the RC frame in the walls. In both cases, light and severe damages and the fragility functions for Dwelling 1 and Dwelling 2 were parallel from each other.

Fig. 8 (c) shows the probability to get collapse of dwellings. Dwelling 1 showed 50% to get damage from 300gals of PGA, while Dwelling 2 from 620gals. In this case, the fragility curves were not parallel, probably due to the good performance of the retrofitted model, which decreased the probability to get damage from small increment of strong ground motion. In other words, for non-retrofitted dwellings, the difference between the strong ground motion that produces severe damage and collapse is small, based on the fact that non-retrofit walls shows sudden collapse due to the crush of the brittle clay tubular bricks.





## 6. Conclusions

Results from experimental tests show that the ductility of non-retrofitted wall, Specimen 1, could be improved by the retrofitting (wire mesh and plaster mortar in two faces of the wall) used in Specimen 2. Also this procedure accomplished the non-crush of clay tubular bricks and increase the capacity of confined masonry, therefore it should be taken into account as a measure to prevent the sudden collapse of confined masonry walls of clay tubular bricks of non-engineered dwellings after a seismic event occurs.

Two kinds of fragility functions have been developed and are proposed to evaluate seismic performance of two stories non-engineered dwellings of clay tubular bricks. The Dwelling 1 considered a dwellings of non-retrofitted walls and Dwelling 2 retrofitted walls. This models were analyzed against the synthetic strong ground motions developed for Lima and scaled for regular soil (S2), according to Peruvian Earthquake Resistant Design NTE-E030-2013, in five stations of the city.

It was estimated that there are 50% probability of collapse for Dwelling 1 based on 300gals of PGA and 620gals for Dwelling 2. Also the fragility functions show for non-retrofitted dwelling model, that the difference between the strong ground motion that produces severe damage and collapse is small, based on the fact that non-retrofitted walls shows sudden collapse due to the crush of the brittle clay tubular bricks. This can be prevented by the use of retrofitting with wire mesh and plaster mortar in two faces of the walls.

The damage level was estimated using the maximum drift based on experimental test data in confined masonry walls of clay solid bricks. Therefore the drift limit for clay tubular bricks are recommended.

## 7. Acknowledgements

The authors would like to express their gratitude to Ministry of Economy and Finance for the financial support on experimental test which was included in the National Budget PP-68.

## 8. References

- [1] Gonzales C., Nakai S, Sekiguchi T, Calderon D, Aguilar Z and Lazares F, (2014): Analysis of Topographic Effects in Dynamic Response of a Typical Rocky Populated Slope in Lima, Peru. *Journal of Disaster Research, Vol.9, No.1*, pp. 17-26.
- [2] National Institute of Statics and Informatics of Peru, INEI.
- [3] Matsuzaki S, Pulido N, Maruyama Y, Estrada M, Zavala C. and Yamazaki F, (2014): Evaluation of Seismic Vulnerability of Buildings Based on Damage Survey Data from the 2007 Pisco, Peru Earthquake, *Journal of Disaster Research Vol.9 No.6*, pp. 1050-1058.
- [4] Quiroz L, Maruyama Y, (2014): Evaluation of seismic performance of residential buildings in Liam, Peru: a case study of building constructed with RC walls and confined masonry walls, *PhD. Master Thesis, Japan*.
- [5] CISMID, (2015): Experimental Study of Mechanicals Properties of Tubular Units without and with retrofit. Program 0068 – Reduction of Vulnerability and Assistant of Emergencies by Disasters, Lima Peru (in Spanish)
- [6] Saito T, (2015): Structural Earthquake Response Analysis 3D, software Stera3D v.4.0, Japan, *Technical Manual*
- [7] Blondet M, (2015): *Construction and maintenance of masonry dwellings, Peru*, 2<sup>nd</sup> edition PUCP (in Spanish)
- [8] SENCICO <http://www.sencico.gob.pe/publicaciones.php?id=228>
- [9] Bommer JJ and Acevedo AB, (2014): The use of real earthquake accelerograms as input to dynamic analysis. *Journal Earthquake Engineering 2004*, 8(4): 1-50.
- [10] Zavala C, Honma C, Gibu P, Gallardo J and Huaco J, (2004): Full scale on line test two story masonry building using hand-made bricks. *13th World Conference on Earthquake Engineering Vancouver, BC, Canada*.